

# Predicting Variation on Void Ratio Deposition Influenced by Hydraulic Conductivity and Porosity Impact in Heterogeneous Silty and Peat Soil Formation



**Jaja GWT and Eluozo SN\***

Department of Civil Engineering, Nigeria

\*Corresponding author: Eluozo SN, Department of Civil Engineering, Faculty of Engineering, Nigeria

Submission: 📅 November 16, 2018; Published: 📅 November 27, 2018

## Abstract

The study predicts the variation of void ratios on hydraulic conductivity and porosity impact for silty and peat sand deposition. The rate conductivity and porosity were considered in the system to predominantly pressure the deposition of void ratio on silty and peat sand formation, such structural deposition experienced predominant heterogeneity in the study location, the deposition reflected unconsolidated deposition that should be evaluated in fundamental analysis of engineering properties of soil for design of foundation, these condition made the study imperative, several experts may always apply the conventional system to generate parameters for void ratio, but the compressive analysis in most time are not gotten, but the analytical techniques applied were able to develop model that can determine the comprehensive deposition of void within the intercedes of the formation, the study has developed another conceptual approach to thoroughly monitor void ratio within silty and peat soil formation.

**Keywords:** Predicting void ratio hydraulic conductivity; Silty and peat sand

## Introduction

current study on nature of soil formations and its engineering stress-strain response Indicate that the soil performs as a collection of scale-level-dependent skeletons arranged in a Particular manner [1-3]. However, several studies have mentioned that the physical nature of silty sand is entirely different from that of clean sand [1,3-7]. They recognized that the undrained residual shear strength (Sus) response depends effectively on the void ratio as a state parameter. It is also anticipated that the global void ratio (e) cannot represent the amount of particle contacts in the sand-silt mixture samples [8-12]. As the void ratio and proportion of the coarse-grained soil or fine-grained soil changes, the nature of their microstructures also changes [13,14]. Due to a large grain size distribution range and availability of voids larger than some grains, at low fines contents, some of the finer grains may remain inactive and swim in the void spaces without affecting or contributing to the force chain [15-17]. Therefore, it is quite important to use new index parameters such as the intergranular [2,18,19]

## Theoretical background

$$K\Phi \frac{d^2e}{dx^2} = DV \frac{de}{dx} + V_{(x)} \frac{de}{dx} \quad (1)$$

$$K\Phi \frac{d^2e}{dx^2} - (DV + V_{(x)}) \frac{de}{dx} \quad (2)$$

$$\text{Let } e = \sum_{n=0}^{\infty} a_n x^n$$

$$e^1 = \sum_{n=1}^{\infty} a_n x^{n-1}$$

$$e^1 = \sum_{n=2}^{\infty} n(n-1)a_n x^{n-2}$$

$$K\Phi \sum_{n=2}^{\infty} n(n-1)a_n x^{n-2} = (D + V_{(x)}) \sum_{n=1}^{\infty} a_n x^{n-1} \quad (3)$$

Replace  $n$  in the 1<sup>st</sup> term by  $n+2$  and in the 2<sup>nd</sup> term by  $n+1$ , so that we have;

$$K\Phi \sum_{n=2}^{\infty} (n+2)(n+1)a_{n+2} x^n = (D + V_{(x)}) \sum_{n=0}^{\infty} (n+1)a_{n+1} x^n \quad (4)$$

$$\text{i.e. } K\Phi (n+2)(n+1)a_{n+2} = (D + V_t)(n+1)a_{n+1} \quad (5)$$

$$a_{n+2} = \frac{(D + V_{(x)})(n+1)a_{n+1}}{K\Phi (n+2)(n+1)} \quad (6)$$

$$a_{n+2} = \frac{(D + V_{(x)})a_{n+1}}{K\Phi (n+2)} \quad (7)$$

$$\text{for } n = 0, a_2 = \frac{(D + V_{(x)})a_1}{2K\Phi} \quad (8)$$

$$\text{for } n = 1, a_3 = \frac{(D + V_t)a_2}{3D} = \frac{(D + V_{(x)})^2 a_1}{2D \cdot 3D} \quad (9)$$

$$\text{for } n = 2; a_4 = \frac{(D + V_{(x)})a_3}{4D} = \frac{(D + V_{(x)})}{4D} \cdot \frac{(D + V_{(x)})a_1}{3D \cdot 2D} = \frac{(D + V_{(x)})^3 a_1}{4D \cdot 3D \cdot 2D} \quad (10)$$

$$\text{for } n = 3; a_3 = \frac{(D_r + V_{(x)})a_4}{5D} = \frac{(D_r + V_{(x)})}{5D \cdot 4D \cdot 3D \cdot 2D} \quad (11)$$

$$\text{for } n; a_n = \frac{(D_r + V_{(x)})^{n-1} a_1}{K\Phi^{n-1} n!} \quad (12)$$

$$C(x) = a_0 + a_1 x + a_2 x^2 + a_3 x^3 + a_4 x^4 + a_5 x^5 + \dots + a_n x_n \quad (13)$$

$$= a_0 + a_1 x + \frac{(D_r + V_{(x)})a_2 x^2}{2!D} + \frac{(D_r + V_{(x)})a_3 x^3}{3!D^2} + \frac{(D_r + V_{(x)})a_4 x^4}{4!D^3} + \frac{(D_r + V_{(x)})a_5 x^5}{5!D^4} + \dots \quad (14)$$

$$C(x) = a_0 + a_1 \left[ x + \frac{(D_r + V_{(x)})x^2}{2!D} + \frac{(D_r + V_{(x)})x^3}{3!D^2} + \frac{(D_r + V_{(x)})x^4}{4!D^3} + \frac{(D_r + V_{(x)})x^5}{5!D^4} \right] \quad (15)$$

$$C(x) = a_0 + a_1 \ell \frac{(D_r + V_{(x)})x}{K\Phi} \quad (16)$$

Subject equation (16) to the following boundary conditions

$$C(0) = 0 \text{ and } C(0) = H$$

$$C(x) = a_0 + a_1 \ell \frac{(D_r + V_{(x)})x}{K\Phi}$$

$$C(0) = a_0 + a_1 = 0$$

$$\text{i.e. } a_0 + a_1 = 0 \quad (17)$$

$$C^1(x) = \frac{(D_r + V_{(x)})}{2!D} a_1 \ell \frac{(D_r + V_{(x)})x}{D}$$

$$C^1(0) = \frac{(D_r + V_{(x)})}{2!D} a_1 = H$$

$$a_1 = \frac{HD}{D_r + V_{(x)}} \quad (18)$$

Substitute (18) into equation (17)

$$a_1 = a_0$$

$$\Rightarrow a_0 = \frac{-H}{D_r - V_{(x)}} \quad (19)$$

Hence the particular solution of equation (16) is of the form:

$$C(x) = \frac{HD}{D_r + V_{(x)}} + \frac{HD}{D_r + V_{(x)}} \ell \frac{(D_r + V_{(x)})x}{D}$$

$$\Rightarrow C(x) = \frac{HD}{D_r + V_{(x)}} \left[ \ell \frac{(D_r + V_{(x)})x}{K\Phi} - 1 \right] \quad (20)$$

## Materials and Method

Standard laboratory experiment where performed to monitor the void Ratio deposition at different formation, the soil deposition of the strata were collected in sequences base on the structural deposition at different study area, this samples collected at different location generate variation at different depth producing different deposition strata void ratio base on their litho structures the experimental result are applied to compare with theoretical values for model validation [20-22].

## Result and Discussion

Results and discussion are presented in Table 1-10 including graphical representation of void ratio at different litho structures. Figure 1-10 shows the deposition of void ratios in linear structural setting as presented in the figures, the depositions of the void ratios within silty and peat formations explain the rate of heterogeneity in deposition of void within the intercede of the formation, the exponential setting from all the graphical representation express the rate of the litho structures of the soil in terms geomorphology effect and geochemistry in the strata depositions, the geological reflection of the location were also observed in the study to pressure the structural setting of the strata. The derived model solution were applied to monitor the depositions as in numerical and analytical setting through simulation, the study has observed the variation of the void from the generated predictive values thus compared with experimental values, it is concluded that the deposition of silty and peat soil in deltaic environment were based on the rate of heterogeneity level of disintegration of the predominant deposited porous rock in deltaic locations. The validation of the simulation developed favourable fits, the derived solution has predicted the void within silty and peat soil formation. The determination of void ratios is basic principle of engineering properties of soil for design of various foundation thus the rate consolidation including settlement of different condition in soil engineering.

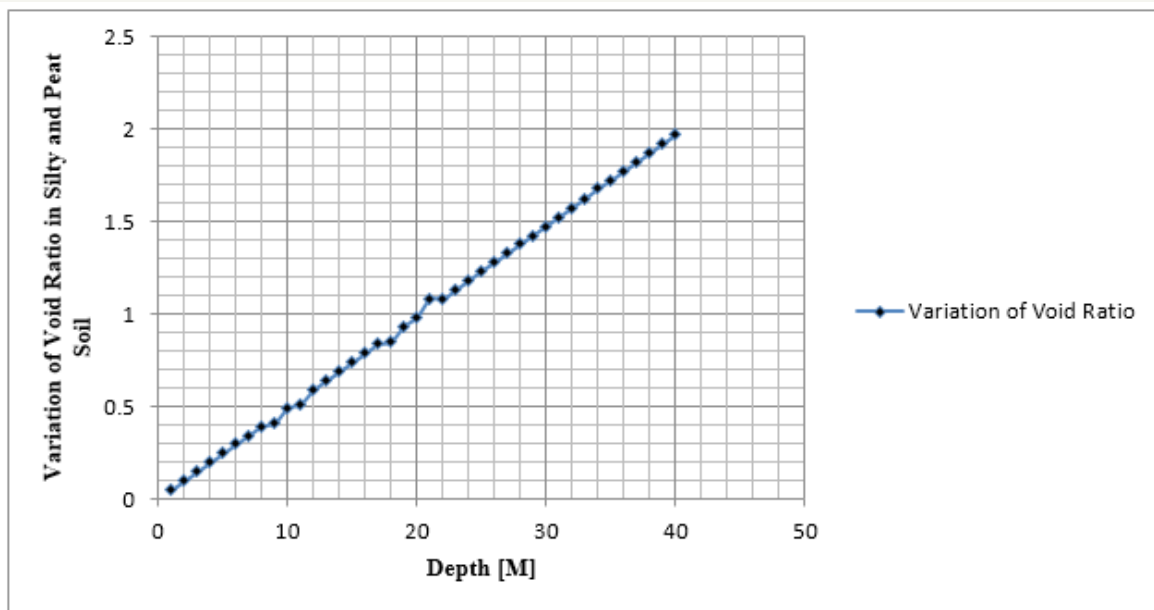


Figure 1: Predictive values of void ratio at different depths.

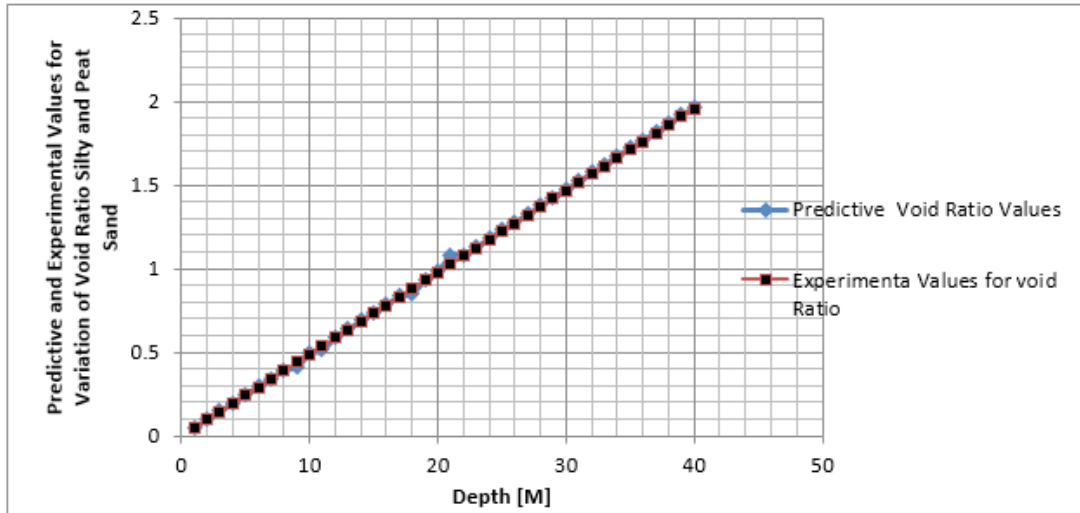


Figure 2: Comparison of predictive and measured values of void ratio at different depth.

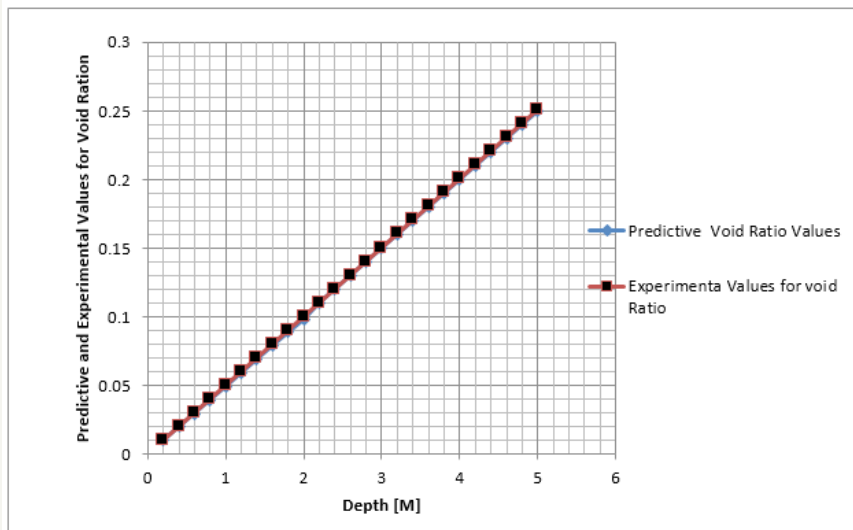


Figure 3: Comparison of predictive and measured values of void ratio at different depth.

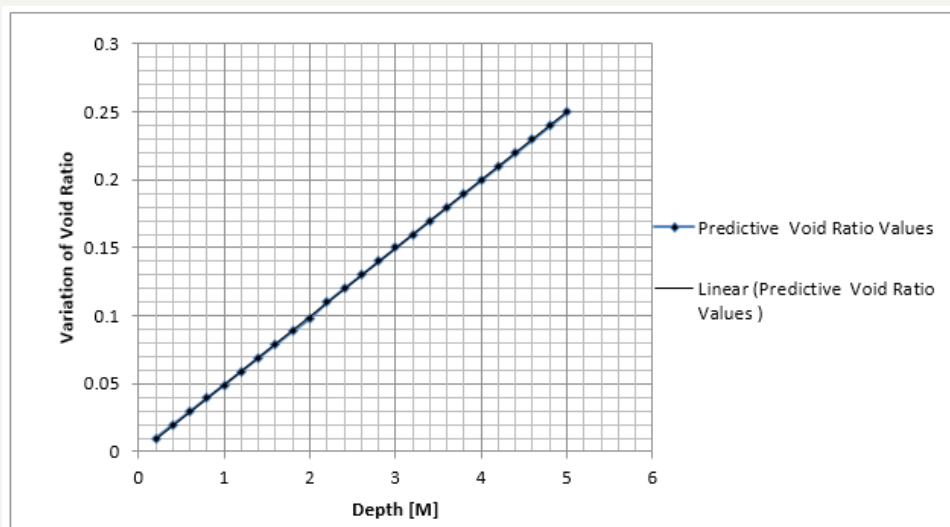


Figure 4: Predictive values of void ratio at different depths.

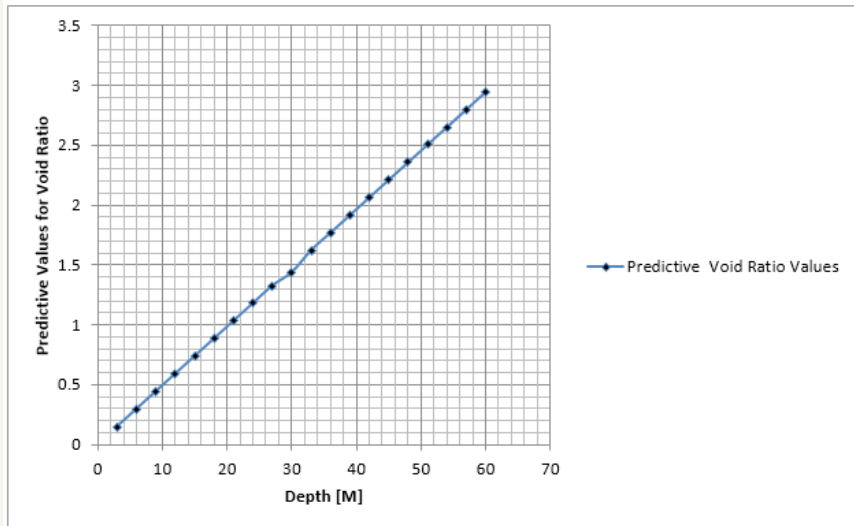


Figure 5: Predictive values of void ratio at different depths.

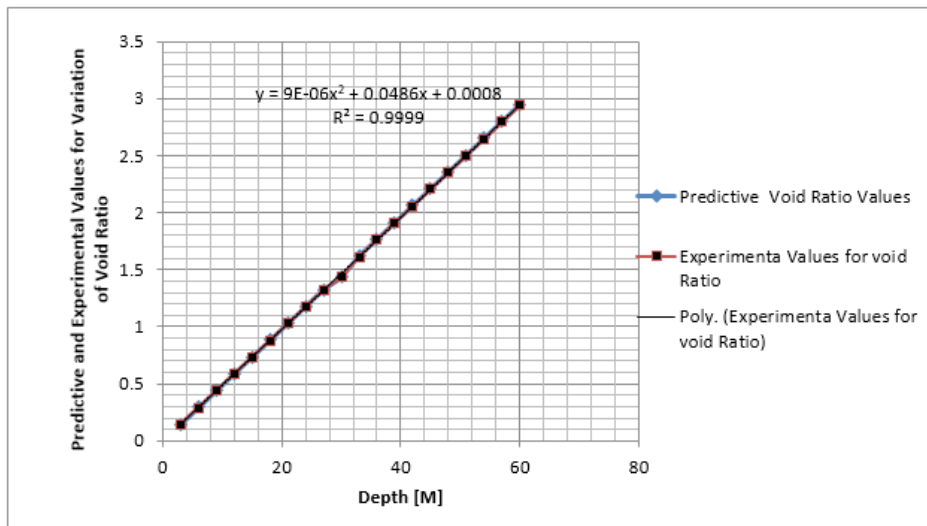


Figure 6: Comparison of predictive and measured values of void ratio at different depth.

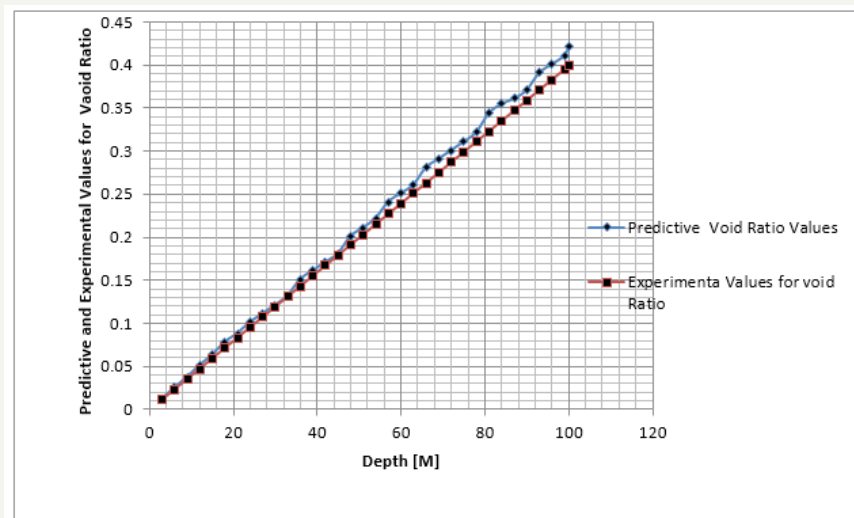


Figure 7: Comparison of predictive and measured values of void ratio at different depth.

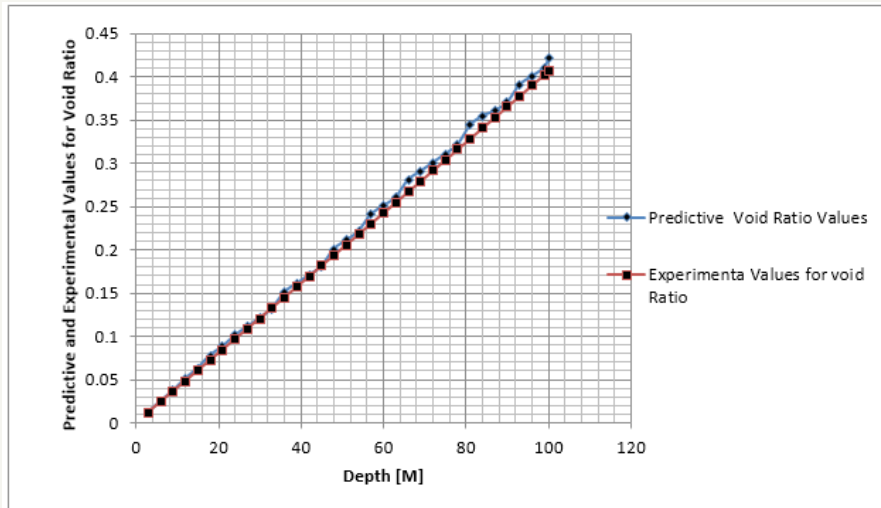


Figure 8: Comparison of predictive and measured values of void ratio at different depth.

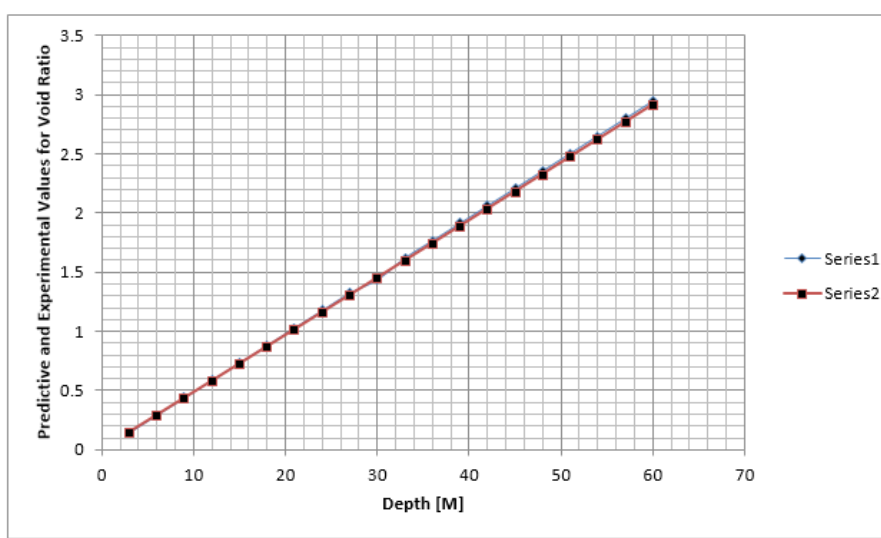


Figure 9: Comparison of predictive and measured values of void ratio at different depth.

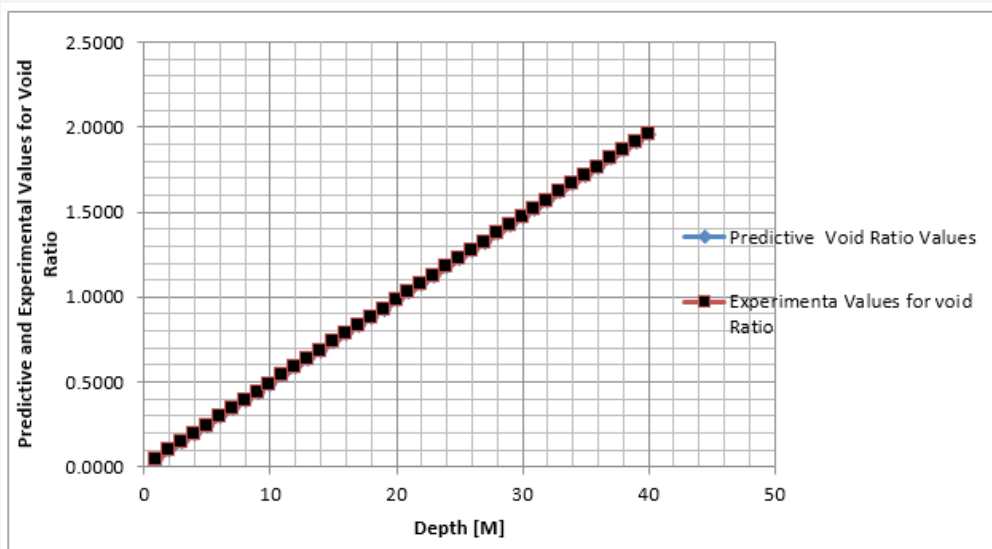


Figure 10: Comparison of predictive and measured values of void ratio at different depth.

**Table 1:** Predictive values of void ratio at different depths.

Depth [M]	Variation of Void Ratio
1	0.0491
2	0.0982
3	0.1476
4	0.1968
5	0.2461
6	0.2962
7	0.3441
8	0.3936
9	0.4123
10	0.4921
11	0.5142
12	0.5904
13	0.6396
14	0.6888
15	0.7381
16	0.7872
17	0.8364
18	0.8523
19	0.9348
20	0.9841
21	1.0822
22	1.0821
23	1.1316
24	1.1808
25	1.2341
26	1.2792
27	1.3284
28	1.3776
29	1.4268
30	1.4761
31	1.5252
32	1.5744
33	1.6236
34	1.6778
35	1.7221
36	1.7712
37	1.8204
38	1.8696
39	1.9188
40	1.9681

**Table 2:** Comparison of predictive and measured values of void ratio at different depth.

Depth [M]	Predictive Void Ratio Values	Experimental Values for void Ratio
1	0.0491	0.0460
2	0.0982	0.0950
3	0.1476	0.1440
4	0.1968	0.1930
5	0.2461	0.2420
6	0.2962	0.2910
7	0.3441	0.3400
8	0.3936	0.3890
9	0.4123	0.4380
10	0.4921	0.4870
11	0.5142	0.5360
12	0.5904	0.5850
13	0.6396	0.6340
14	0.6888	0.6830
15	0.7381	0.7320
16	0.7872	0.7810
17	0.8364	0.8300
18	0.8523	0.8790
19	0.9348	0.9280
20	0.9841	0.9770
21	1.0822	1.0260
22	1.0821	1.0750
23	1.1316	1.1240
24	1.1808	1.1730
25	1.2341	1.2220
26	1.2792	1.2710
27	1.3284	1.3200
28	1.3776	1.3690
29	1.4268	1.4180
30	1.4761	1.4670
31	1.5252	1.5160
32	1.5744	1.5650
33	1.6236	1.6140
34	1.6778	1.6630
35	1.7221	1.7120
36	1.7712	1.7610
37	1.8204	1.8100
38	1.8696	1.8590
39	1.9188	1.9080
40	1.9681	1.9570

**Table 3:** Comparison of predictive and measured values of void ratio at different depth.

Depth [M]	Predictive Void Ratio Values	Experimental Values for Void Ratio
0.2	0.00984	0.010002
0.4	0.0197	0.020008
0.6	0.0295	0.030018
0.8	0.0394	0.040032
1	0.049	0.05005
1.2	0.059	0.060072
1.4	0.069	0.070098
1.6	0.0788	0.080128
1.8	0.0886	0.090162
2	0.098	0.1002
2.2	0.11	0.110242
2.4	0.12	0.120288
2.6	0.13	0.130338
2.8	0.14	0.140392
3	0.15	0.15045
3.2	0.16	0.160512
3.4	0.17	0.170578
3.6	0.18	0.180648
3.8	0.19	0.190722
4	0.2	0.2008
4.2	0.21	0.210882
4.4	0.22	0.220968
4.6	0.23	0.231058
4.8	0.24	0.241152
5	0.25	0.25125

**Table 4:** Predictive values of void ratio at different depths.

Depth [M]	Predictive Void Ratio Values
0.2	0.00984
0.4	0.0197
0.6	0.0295
0.8	0.0394
1	0.049
1.2	0.059
1.4	0.069
1.6	0.0788
1.8	0.0886
2	0.098
2.2	0.11
2.4	0.12
2.6	0.13
2.8	0.14
3	0.15
3.2	0.16
3.4	0.17
3.6	0.18
3.8	0.19
4	0.2
4.2	0.21
4.4	0.22
4.6	0.23
4.8	0.24
5	0.25

**Table 5:** Predictive values of void ratio at different depths.

Depth [M]	Predictive Void Ratio Values
3	0.147
6	0.294
9	0.441
12	0.589
15	0.736
18	0.883
21	1.031
24	1.178
27	1.325
30	1.437
33	1.621
36	1.767
39	1.914
42	2.062

45	2.209
48	2.356
51	2.504
54	2.651
57	2.798
60	2.946

**Table 6:** Comparison of predictive and measured values of void ratio at different depth.

Depth [M]	Predictive Void Ratio Values	Experimental Values for Void Ratio
3	0.147	0.145
6	0.294	0.292
9	0.441	0.439
12	0.589	0.586
15	0.736	0.733
18	0.883	0.881
21	1.031	1.027
24	1.178	1.175
27	1.325	1.322
30	1.437	1.435
33	1.621	1.615
36	1.767	1.765
39	1.914	1.912
42	2.062	2.059
45	2.209	2.207
48	2.356	2.354
51	2.504	2.502
54	2.651	2.649
57	2.798	2.796
60	2.946	2.944

**Table 7:** Comparison of predictive and measured values of void ratio at different depth.

Depth [M]	Predictive Void Ratio Values	Experimental Values for Void Ratio
3	0.012	0.011
6	0.025	0.023
9	0.037	0.035
12	0.051	0.047
15	0.063	0.059
18	0.078	0.071
21	0.088	0.083
24	0.101	0.095
27	0.111	0.107
30	0.121	0.119
33	0.132	0.131
36	0.151	0.143
39	0.161	0.155
42	0.171	0.167
45	0.181	0.179



48	0.201	0.191
51	0.211	0.203
54	0.222	0.215
57	0.241	0.227
60	0.251	0.239
63	0.261	0.251
66	0.281	0.263
69	0.291	0.275
72	0.301	0.287
75	0.311	0.299
78	0.322	0.311
81	0.344	0.323
84	0.355	0.335
87	0.361	0.347
90	0.371	0.359
93	0.391	0.371
96	0.401	0.383
99	0.411	0.395
100	0.421	0.399

**Table 8:** Comparison of predictive and measured values of void ratio at different depth.

Depth [M]	Predictive Void Ratio Values	Experimental Values for Void Ratio
3	0.012	0.0120063
6	0.025	0.0240252
9	0.037	0.0360567
12	0.051	0.0481008
15	0.063	0.0601575
18	0.078	0.0722268
21	0.088	0.0843087
24	0.101	0.0964032
27	0.111	0.1085103
30	0.121	0.12063
33	0.132	0.1327623
36	0.151	0.1449072
39	0.161	0.1570647
42	0.171	0.1692348
45	0.181	0.1814175
48	0.201	0.1936128
51	0.211	0.2058207
54	0.222	0.2180412
57	0.241	0.2302743
60	0.251	0.24252
63	0.261	0.2547783
66	0.281	0.2670492
69	0.291	0.2793327
72	0.301	0.2916288

75	0.311	0.3039375
78	0.322	0.3162588
81	0.344	0.3285927
84	0.355	0.3409392
87	0.361	0.3532983
90	0.371	0.36567
93	0.391	0.3780543
96	0.401	0.3904512
99	0.411	0.4028607
100	0.421	0.407

**Table 9:** Comparison of predictive and measured values of void ratio at different depth.

Depth [M]	Predictive Void Ratio Values	Experimental Values for Void Ratio
3	0.147	0.144081
6	0.294	0.288324
9	0.441	0.432729
12	0.589	0.577296
15	0.736	0.722025
18	0.883	0.866916
21	1.031	1.011969
24	1.178	1.157184
27	1.325	1.302561
30	1.437	1.4481
33	1.621	1.593801
36	1.767	1.739664
39	1.914	1.885689
42	2.062	2.031876
45	2.209	2.178225
48	2.356	2.324736
51	2.504	2.471409
54	2.651	2.618244
57	2.798	2.765241
60	2.946	2.9124

**Table 10:** Comparison of predictive and measured values of void ratio at different depth.

Depth [M]	Predictive Void Ratio Values	Experimental Values for Void Ratio
1	0.0460	0.046
2	0.0950	0.095
3	0.1440	0.144
4	0.1930	0.193
5	0.2420	0.242
6	0.2910	0.291
7	0.3400	0.34
8	0.3890	0.389
9	0.4380	0.438
10	0.4870	0.487

11	0.5360	0.536
12	0.5850	0.585
13	0.6340	0.634
14	0.6830	0.683
15	0.7320	0.732
16	0.7810	0.781
17	0.8300	0.83
18	0.8790	0.879
19	0.9280	0.928
20	0.9770	0.977
21	1.0260	1.026
22	1.0750	1.075
23	1.1240	1.124
24	1.1730	1.173
25	1.2220	1.222
26	1.2710	1.271
27	1.3200	1.32
28	1.3690	1.369
29	1.4180	1.418
30	1.4670	1.467
31	1.5160	1.516
32	1.5650	1.565
33	1.6140	1.614
34	1.6630	1.663
35	1.7120	1.712
36	1.7610	1.761
37	1.8100	1.81
38	1.8590	1.859
39	1.9080	1.908
40	1.9570	1.957

## Conclusion

The prediction of void ratios for silty and peat soil formation was to determine the heterogeneity of void ratios in peat and silty depositions under the influences of hydraulic conductivities and porosities in silty and peat sand depositions. The study tries to predict the structural deposition of silty and peat through their disintegration from predominant porous rock in deltaic environment, from the graphical representations, it was observed that the structures of the formations experiences linear depositions from the made soil to peat soil. Void ratios were in heterogeneity in exponential setting observed from graphical representations, this implies that the litho structures were influenced by the level of disintegration in the porous rock under the influences from variations of porosities and hydraulic conductivities, the derived solution were subjected to simulation, the validation generated favourable fits, these explain the void ratios within silty and peat soil depositions in deltaic environment. The basic principles in engineering properties of soil mechanics has been developed

applying this analytical or deterministic modelling techniques. This can be applied to determine void ratios in settlements or any other design of foundation system.

## References

1. Thevanayagam S (1997) Dielectric dispersion of porous media as a fractal phenomenon. *J of Applied Physics* 82(5): 2538-2547.
2. Thevanayagam S (1998) Effect of fines and confining stress on undrained shear strength of silty sands. *J Geotech Geoenviron Eng Div* 124(6): 479-491.
3. Mostefa B, Hanifi M, Ahmed A, Nouredine D, Tom S (2011) Undrained shear strength of sand-silt mixture: Effect of intergranular void ratio and other parameters. *KSCE Journal of Civil Engineering* 15(8): 1335-1342.
4. Zlatovic S, Ishihara K (1995) On the influence of non-plastic fines on residual strength. *Proc. of the first Int Conf on Earthquake Geotech Eng, Tokyo*, pp. 14-16.
5. Lade PV, Yamamuro JA (1997) Effects of non-plastic fines on static liquefaction of sands. *Canadian Geotech J* 34(6): 918-928.
6. Amini F, Qi GZ (2000) Liquefaction testing of stratified silty sands. *J of Geotech Geoenviron Eng Proc* 26(3): 208-217.

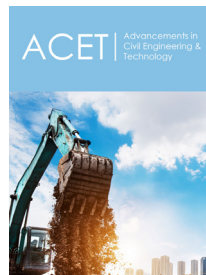
7. Naeini SA, Baziar MH (2004) Effect of fines content on steady-state strength of mixed and layered samples of a sand. *Soil Dyna and Earth Eng* 3: 181-187.
8. Eluozo SN, Ode T (2015) Mathematical model to predict compression index of uniform loose sand in coastal area of Degema, rivers state of Nigeria. *International Journal of Advance Research in Engineering and Technology* 6(12): 86-103.
9. Eluozo SN, Ode T (2015) Mathematical to monitor stiff clay compression index in wet land area of Degema. *International Journal of Advance Research in Engineering and Technology* 6(12): 59-72.
10. Ode T, Eluozo SN (2016) Predictive model on compressive strength of concrete made with locally 3/8 Gravel from different water cement ratios and curing age. *International Journal of Scientific and Engineering Research* 7(1): 1528-1551.
11. Ode T, Eluozo SN (2016) Model prediction to monitor the rate of water absorption of concrete pressured by variation of time and water cement ratios. *International Journal of Scientific and Engineering Research* 7(1): 1514-1527
12. Ode T, Eluozo SN (2016) Calibrating the density of concrete from washed and unwashed locally 3/8 gravel material at various curing age. *International Journal of Scientific and Engineering Research* 7(1): 1514-1552.
13. Thevanayagam S, Mohan S (2000) Inter-granular state variables and stress-strain behaviour of silty sands. *Geotechnique* 50(1): 1-23.
14. Thevanayagam S, Ravishankar K, Mohan S (1997) Effects of fines on monotonic undrained shear strength of sandy soils. *AST Geotech Testing J* 20(1): 394-406.
15. Ode T, Eluozo SN (2016) Compressive strength calibration of washed and unwashed locally occurring 3/8 gravel from various water cement ratios and curing age. *International Journal Engineering and General Science* 4(1): 462-483.
16. Ode T, Eluozo SN (2016) Predictive model to monitor variation of concrete density influenced by various grade from locally 3/8 gravel at different curing time. *International Journal Engineering and General Science* 4(1): 502-522.
17. Ode T, Eluozo SN (2016) Predictive model to monitor vitiation of stress-strain relationship of 3/8 gravel concrete with water cement ration [0.45] at different load. *International Journal Engineering and General Science* 4(1): 409-418.
18. Monkul MM (2005) Influence of inter-granular void ratio on one dimensional compression, M. Sc. Thesis, Dokuz Eylul University, Izmir, Turkey.
19. Eluozo SN, Ode T (2016) Modeling and simulation on velocity and permeability to predict bacillus on lag phase in predominant lateritic and silty formation in coastal area of Abonnema, Niger delta of Nigeria. *International Journal of Civil Engineering and Technology* 7(1): 304-314.
20. Baziar MH, Dobry R (1995) Residual strength and large-deformation potential of loose silty sands. *J of Geotech Eng* 121: 896-906.
21. Ladd RS (1978) Preparing test specimen using under compaction. *Geotech Testing J* 1(1): 16-23.
22. Thevanayagam S, Nesarajah S (1998) Fractal model for flow through saturated soil. *Journal of Geotechnical and Geoenvironmental Engineering* 124(1): 53-66.



Creative Commons Attribution 4.0  
International License

For possible submissions Click Here

[Submit Article](#)



### Advancements in Civil Engineering & Technology

#### Benefits of Publishing with us

- High-level peer review and editorial services
- Freely accessible online immediately upon publication
- Authors retain the copyright to their work
- Licensing it under a Creative Commons license
- Visibility through different online platforms